Desalination and Water Treatment
www.deswater.com

doi: 10.5004/dwt.2020.24871

180 (2020) 336–348
March

Enhancement of adsorption characteristics of Methyl violet 2B dye through NaOH treatment of *Cucumis melo var. cantalupensis* (rock melon) skin

Linda B.L. Lim[a,*], Namal Priyantha[b,c], Xiao Han Bong[a], Nur Afiqah Hazirah Mohamad Zaidi[a]

[a]*Department of Chemistry, Faculty of Science, Universiti Brunei Darussalam, Jalan Tungku Link, Gadong, Negara Brunei Darussalam, Tel. +673-8748010; emails: linda.lim@ubd.edu.bn (L.B.L. Lim), xiaohan6229@hotmail.com (X.H. Bong), afhazirah@gmail.com (N.A.H. Mohamad Zaidi)*
[b]*Department of Chemistry, Faculty of Science, University of Peradeniya, Peradeniya, Sri Lanka, email: namal.priyantha@yahoo.com*
[c]*Postgraduate Institute of Science, University of Peradeniya, Peradeniya, Sri Lanka*

Received 12 February 2019; Accepted 8 September 2019

ABSTRACT

A new adsorbent derived from the skin of *Cucumis melo var. cantalupensis* (CMS) through surface modification with 1 M NaOH (MCMS) was investigated for its enhanced ability to adsorb methyl violet 2B (MV 2B) dye. The optimum contact time for both CMS and MCMS to reach equilibrium was at 90 min. The effect of pH indicated that dye removal at higher pH was comparable with the untreated pH. The pseudo-second-order model best described the adsorption kinetics data for both CMS and MCMS. The Sips isotherm model fitted the adsorption process with maximum adsorption capacity (q_{max}) of 224.56 and 669.73 mg g^{-1} for CMS and MCMS, respectively, indicating that simple surface modification of CMS with NaOH significantly enhanced the adsorption capacity of the adsorbent toward MV 2B by approximately 200%. Further, it is found that the removal of MV 2B by MCMS was not affected by ionic constituents as much as CMS, demonstrating the superior characteristics of MCMS. Regeneration and reuse of both spent adsorbents are possible, especially when washed with acid. Overall, based on the high q_{max} values as compared with those of many reported adsorbents, both CMS and MCMS are potentially strong adsorbents for the removal of MV 2B dye in real-life wastewater treatment.

Keywords: Rock melon skin; Adsorbent; Methyl violet dye; Surface modification; Adsorption isotherm

1. Introduction

A major concern encountered by most countries is related to environmental issues. As water is one of the most important basic needs in life, contamination of the water sources is taken seriously to ensure that the water quality is maintained at a standard level. However, development of large-scale industries and expansion of service activities have drastically worsened the quality of water [1]. Sources of water pollution include effluents from industrial wastes, oil spillage, radioactive wastes, sewage and many others [2]. Therefore, proper wastewater management is crucial in controlling water pollution.

The rising of textile industry has created a massive problem in water pollution as the by-products of the industry are the most chemically intensive. Since different types of chemicals are used during the production of fabrics, such as dyeing and printing, there is a high possibility that chemicals used by the industries be directly or indirectly disposed into water ways without proper pre-treatment to remove toxic constituents. Furthermore, large amounts of water are required by the textile industry for the production process,

* Corresponding author.

such as printing, dyeing and processing [3]. Hence, it appears that textile industry could be one of the major contributors to water pollution [4]. This fact is supported by encountering serious water pollution issues generated by textile industry in India, a newly industrialized nation [5]. In aiming to reduce the effect of water pollution and wastewater coming from textile industry, new technologies should be introduced to encounter the problems raised [6].

Some dyes being used for dyeing operations can be toxic pollutants as they could produce harmful effects on both environment and human health [7–10]. Many synthetic dyes are non-biodegradable, toxic, and are highly visible [11,12]. Generally, wastewater containing dye pollutants shows high biochemical oxygen demand (BOD), and is very rich in color. One of the consequences of dye pollutants is the depletion of dissolved oxygen levels which is a basic need for the survival of aquatic organisms. Furthermore, dyes may prevent light from reaching the aquatic organisms, leading to an imbalance of ecosystem and making drinking water unsafe to consume. Hence, it is important that effective solutions on the treatment of dye-polluted wastewater be searched upon.

Methyl violet 2B (MV 2B) dye is a basic dye which is highly visible and commonly used in the textile industry. Health effects such as eyes and skin damages, and carcinogenic characteristics can be resulted from ingestion or inhalation of MV 2B dyes [13]. Furthermore, it has been reported that MV 2B dye could affect the growth of aquatic organisms and bacteria [14]. Owing to the above factors, there is a need in removing MV 2B dye from wastewater. Adsorption method is used in this study as it is one of the most simple, cheap and cost-effective treatment methods [15]. This method is also significant as it does not produce any by-products causing harmful effects to the environment and also human health [16].

A new adsorbent, that is, skin derived from *Cucumis melo var. cantalupensis* (CMS), or commonly known as rock melon, was investigated for its adsorption potential toward MV 2B. According to the United States Department of Agriculture (USDA) report, domestic consumption of fruits and vegetables increases annually and melons are one of the main contributions to the growth per person annually [17]. As the demand for fruits increases, skin of fruits as an agriculture waste will result in a large contribution to landfill waste. Although rock melon is a popular fruit, the skin is of no economic value and thrown away as waste. Hence utilizing the skin is a twofold advantage in terms of contributing to reduce the landfill waste produced by it, and at the same time, it helps remove toxic MV 2B from wastewater. CMS was also modified by using a base, NaOH. This is because various studies have shown that chemical modification of low-cost adsorbents can be found to either enhance or possibly reduce the adsorption capacity on the removal of pollutants [18–21]. Chemical modification is a method which changes the surface of an adsorbent by adding new functional groups to the surface which allow more molecules to be attached onto it through chemical and physical interactions. Some modification can also improve the porosity of the adsorbent's surface, hence, enhances the adsorption efficiency of the adsorbent [22].

The adsorption characteristics of both untreated and base-modified CMS, which included the main factors that influence the effectiveness of adsorption such as the effects of medium pH, temperature, contact time and presence of salts, were studied using batch adsorption experiments. Other studies included adsorption isotherm and kinetic mechanisms of the interactions between adsorbent and adsorbate. Regeneration studies were carried out to determine if the spent adsorbents could be regenerated and reused. Finally, both the adsorbents were characterized. Therefore, the parameters listed would provide insight as to whether the adsorbents (CMS and MCMS) are suitable as potential new adsorbents to remove MV 2B dye effectively. Comparison will be made between CMS and MCMS and also with adsorbents from other literature reviews to provide an idea on the adsorption ability toward MV 2B dye.

2. Materials and methods

2.1. Chemicals and reagents

The dye used in this study was methyl violet 2B (MV 2B), with molecular formula $C_{23}H_{26}N_3Cl$ and Mr: 393.96 g mol^{-1}. A 1,000 mg L^{-1} stock solution of MV 2B dye was prepared by dissolving 1.0 g of dye in 1,000 mL of distilled water. Lower concentrations were prepared from the stock solution by serial dilution. The pH of solutions was adjusted using 0.1 M HCl and/or 0.1 M NaOH. Four salts purchased from GPR (UK) (NaCl), Fluka (USA) (KCl) and Merck (USA) (KNO_3 and $NaNO_3$) were used in the determination of the effect of ionic strength on MV 2B removal.

2.2. Preparation of the adsorbents

Cucumis melo var. cantalupensis was purchased from the local market in the Brunei-Muara District in Brunei Darussalam. The skin of the fruit (CMS) was separated from its edible flesh and was washed with distilled water to remove any surface impurities. CMS was then dried at 60°C for a week, ground into powder, and sieved using a 380 μm metal sieve. Powdered CMS of particle size <380 μm was used in all subsequent experiments.

2.3. Surface modification of the adsorbent

CMS was shaken in 1.0 M NaOH in the ratio of 1.0 g:20.0 mL for 2.0 h. The surface-modified CMS (MCMS) was filtered and washed with distilled water several times until a neutral pH was obtained. The MCMS was then dried at 60°C and stored in an air-tight glass bottle until further use.

2.4. Instrumentation

The absorbance of MV 2B dye was measured using the Shimadzu UV 1601 UV-Visible spectrophotometer (Japan) at a wavelength of 584 nm. The JSM-7610F Field Emission Scanning Electron Microscope was used to obtain the surface morphology of both CMS and MCMS. The functional groups of CMS and MCMS were determined using the Agilent Cary 630 FTIR spectrometer (USA). To determine pH of solutions, GP 353 ATC pH meter was used. All solutions were agitated at 250 rpm using a Stuart orbital shaker or thermo shaker at ambient temperature.

2.5. Optimization of parameters

2.5.1. Contact time

The investigation of contact time required for the adsorbent–adsorbate system to reach equilibrium was carried out using 0.050 g of adsorbent in 25.0 mL of 500 mg L^{-1} adsorbate, followed by agitation. At every 0.5 h interval, one flask was removed and the solution was filtered using a metal sieve and this was continued up to a total of 4.0 h. Dye contents in filtrates were determined at 584 nm.

2.5.2. Medium pH

An adsorbent sample of 0.050 g was added to each flask containing 25.0 mL of 100 mg L^{-1} MV 2B dye with different pH ranging from 2 to 10. The mixtures were agitated for the optimum contact time period. The solutions were filtered and the absorbance of the filtrates was recorded.

2.5.3. Ionic strength

A sample of 0.050 g of adsorbent was added to an aliquot of 25.0 mL of 100 mg L^{-1} of MV 2B dye solution prepared separately in four salt solutions (NaCl, KCl, $NaNO_3$, KNO_3) of different concentrations (0.01, 0.1, 0.2, 0.4, 0.6, 0.8, and 1.0 mol L^{-1}). The mixtures were agitated for the optimum contact time period. The solutions were filtered and the absorbance values of filtrates were recorded.

2.6. Batch adsorption studies

2.6.1. Adsorption isotherms

Batch adsorption isotherm studies were conducted using 0.050 g of adsorbent in a series of 25.0 mL of MV 2B dye solutions of different concentrations (0–1,000 mg L^{-1} for unmodified CMS, 0–2,000 mg L^{-1} for MCMS). After shaking the mixtures for the optimum time period, the solutions were filtered and the absorbance values of filtrates were recorded.

2.6.2. Kinetic studies

Kinetic studies were carried out using 0.050 g of adsorbent in 25.0 mL of MV 2B dye at two different concentrations (100 and 500 mg L^{-1}). Shaking of the adsorbent–adsorbate mixtures was carried out for the optimum contact time period at 250 rpm at ambient temperature. Solutions were withdrawn at 3 min intervals for the first 30, 10 min intervals for the next 30 and 30 min intervals thereafter. The solutions were filtered and the absorbance values of filtrates were determined.

2.7. Regeneration studies

Regeneration of adsorbent was carried out using four different treatment methods: quick wash, distilled water, acid wash (0.1 mol L^{-1} of HCl) and base wash (0.1 mol L^{-1} of NaOH). CMS and MCMS were each divided into five sets treated with 800 and 2,000 mg L^{-1} of MV 2B dyes, respectively, with a ratio of 1 g:500 mL. The mixtures were agitated for the optimum contact time period. The residues of MV-adsorbent were dried and desorption was carried out through different treatment methods stated above with a ratio of 1 g:50 mL for 2.0 h, followed by multiple washing with distilled water until neutral pH was obtained. The residues were then dried until the next cycle. The procedure of shaking with dye and washing was considered as one cycle. The same procedure of adsorption–desorption process was carried out with different solutions until five cycles were reached.

2.8. Point of zero charge

Point of zero charge was carried out using 0.050 g of adsorbent in 25.0 mL of 0.1 M KNO_3 solution with different pH ranging from 2 to 10. The mixtures were shaken for 24 h, solutions were filtered and the final pH of each filtrate was determined.

3. Results and discussion

3.1. Effect of contact time

Experiments were carried out in order to find the effect of contact time on how fast the adsorbent–adsorbate system reaches equilibrium. It is observed from Fig. 1 that both CMS and MCMS showed a similar trend where there was a rapid removal of MV 2B dye during the initial stage from 0 to 0.5 h attributing to the unoccupied active sites on the surface of the adsorbents being readily available for adsorption. Thereafter, as more sites are being occupied by dye molecules, the adsorbents quickly became saturated and eventually reached equilibrium, as indicated by the plateau. Both CMS and MCMS showed that the highest percentage of dye removal was at 1.5 h, which was taken as the optimum shaking time. It is observed from Fig. 1 that the overall percentage removal of dye by MCMS is much higher than that of CMS.

3.2. Effect of pH

Acidity of an adsorbate greatly influences the adsorption process by affecting electrostatic interactions between the adsorbate and adsorbent. At pH 2, the removal of dyes was at its lowest (Fig. 2). Under acidic condition, protonation causes the adsorbent's surface to be predominantly positive. Hence, MV 2B being a cationic dye experiences high electrostatic repulsion with the adsorbent, resulting in lower removal of

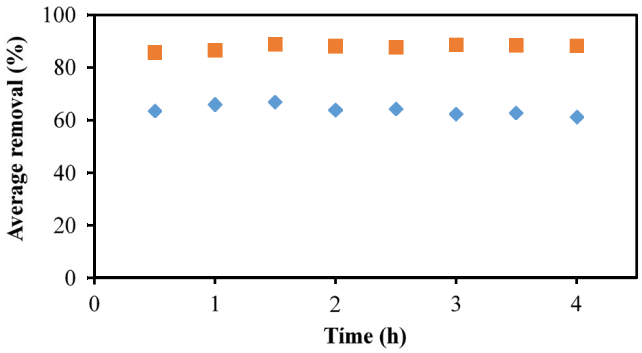

Fig. 1. Effect of contact time on adsorption of MV 2B onto CMS (◆) and MCMS (■).

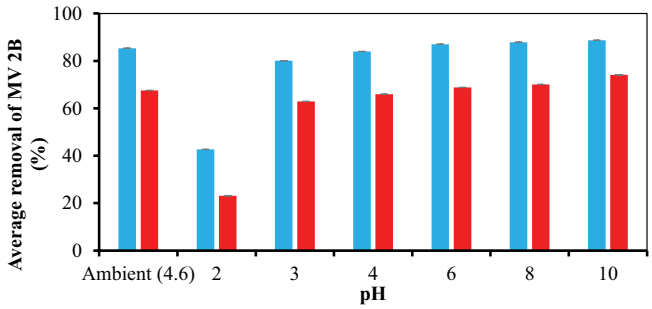

Fig. 2. Effect of pH on the adsorption of MV 2B onto CMS (■) and MCMS (■).

dye. The presence of high concentration of H^+ ions also results in competition between these ions and the cationic MV 2B dye for the active sites on the adsorbent's surface. The reverse effect is observed as the pH increased from 3 to 10, within which the percentage removal of dyes increased gradually.

Another noticeable observation from Fig. 2 is that the percentage removal of MV 2B dye by MCMS is higher than that of CMS. Base modification of CMS resulted in deprotonation of the surface functional groups and also caused hydroxyl ions to attach to the surface of CMS. The increase in the surface's negativity effectively increases the adsorption efficiency toward cationic MV 2B dye. Since the removal of MV 2B dye at unadjusted (ambient) pH is comparable with those in higher pH, adjustment of pH was deemed unnecessary, and hence, all subsequent experiments were carried out at ambient pH. It should be stressed that optimization of medium pH would be essential in extending such studies to real-life situation with large volumes of the dye.

3.3. Adsorption isotherms

Isotherm studies were carried out to determine how an adsorbate in an adsorption process depends on the adsorbate concentration [23]. Six isotherm models were used to analyze experimental data obtained, namely the Langmuir [24], Freundlich [25], Temkin [26], Dubinin–Radushkevich (D-R) [27], Redlich–Peterson (R-P) [28] and Sips [29].

The assumptions of the Langmuir isotherm are that adsorption takes place on the homogeneous surface of the adsorbent forming a monolayer. As the active sites are only on the first layer of the adsorbent, there will be no interaction occurring on the inner surface of the adsorbate [24]. The Langmuir model provides good explanation on the adsorption process for adsorbate at high concentration. The linear equation of the Langmuir isotherm model is given in Eq. (1).

$$\frac{C_e}{q_e} = \frac{1}{q_m} C_e + \frac{1}{K_L \times q_m} \tag{1}$$

The Freundlich isotherm assumes that adsorption takes place on a heterogeneous surface of the adsorbent with the formation of multi-layers. The Freundlich model explains better on adsorption of low concentration adsorbate. The linear equation of the Freundlich isotherm model is expressed in Eq. (2).

$$\ln q_e = \ln K_F + \frac{1}{n} \ln C_e \tag{2}$$

The Temkin isotherm model accounts for the heat of the adsorption process with surface interaction between adsorbent and adsorbate. The expression of the Temkin isotherm model is shown in Eq. (3).

$$q_e = \frac{RT}{b_T} \ln\left(K_T C_e\right) \tag{3}$$

A simplified linear equation of Temkin isotherm is given in Eq. (4):

$$q_e = \beta \ln a + \beta \ln C_e \tag{4}$$

where

$$\beta = \frac{RT}{b_T} \tag{5}$$

The Dubinin–Radushkevich (D-R) isotherm model on microporous adsorption rather than physical adsorption determines the free energy of adsorption. This model only applies for adsorbate with intermediate concentration at low pressure. The linear equation of D-R model is shown in Eq. (6).

$$\ln q_e = q_{\max} \exp\left(-\beta \varepsilon^2\right) \tag{6}$$

where $\varepsilon = RT \ln\left(1 + \frac{1}{C_e}\right)$ and Free energy $(E) = \frac{1}{\sqrt{2\beta}}$.

The Redlich–Peterson (R-P) model is a three-parameter isotherm model applied to both homogenous and heterogeneous surfaces of an adsorbent. The R-P model is a combination of the Langmuir and Freundlich isotherm models. It follows the Langmuir at low concentration and the Freundlich at high concentration. Therefore, the R-P isotherm model, as expressed in the linear from in Eq. (7), can cover a wide range of adsorbate concentration.

$$\ln\left[\frac{K_R C_e}{q_e} - 1\right] = \ln a_R + \beta_R \ln C_e \tag{7}$$

The Sips isotherm model is also a combination of the Langmuir and the Freundlich isotherm models. At low concentration, it reduces to the Freundlich model but at high concentration it follows the Langmuir isotherm model. Eq. (8) is used in the Sips isotherm model.

$$q_e = \frac{K_s C_e^{\beta s}}{1 - a_s C_e^{\beta s}} \tag{8}$$

Linear equation of the Sips isotherm model (Eq. (9)) is shown below:

$$\beta_s \ln C_e = -\ln \frac{K_s}{q_e} + \ln a_s \quad (9)$$

Fig. 3 shows the experimental data obtained for the adsorption isotherms of both CMS and MCMS. The main difference between the two adsorbents is in the concentration of MV 2B dye for each of the system to reach equilibrium. The adsorption capacity of CMS increased, as expected, reaching the saturation point at 700 mg L^{-1}. However, MCMS reached a much higher adsorption capacity before becoming saturated at around 2,000 mg L^{-1}. This indicates that MCMS was able to adsorb MV 2B dye at a much higher concentration as compared with that of CMS. Enhancement of adsorption capacity of CMS toward MV 2B dye through NaOH modification is thus convinced.

Table 1 shows the parameter values obtained for all the adsorption models used in this study. To determine the best fit isotherm model for the removal of MV 2B dye by CMS and MCMS, three different criteria were employed. First, comparison was made between the experimental data with each isotherm model, as shown by the simulation plots in Figs. 3a and b for CMS and MCMS, respectively. Two other criteria used were based on the highest R^2 obtained from the linear plots of the isotherm models and the lowest errors were based on six different error functions as shown in Table 2.

The simulation plots in Fig. 4 for the removal of MV 2B dye by CMS and MCMS show very clearly that the D-R, R-P and Freundlich isotherm models deviated the most from the experimental data. Hence, these models are unsuitable to describe the adsorption isotherm of MV 2B dye. This can be further confirmed by low R^2 and high error values, especially for the R-P and D-R models, as shown in Table 3.

Overall, the results show that the Sips isotherm with the highest R^2 value closest to 1 and lowest errors is the most suitable model which fitted the experimental data for both CMS and MCMS. The Sips represents both the Langmuir and Freundlich models, and for adsorbate of low concentration, the adsorption follows the Freundlich isotherm while for adsorbate of high concentration, adsorption follows the Langmuir isotherm model.

Table 4 shows different types of adsorbents reported for the removal of MV 2B dye. Adsorption capacity of CMS is higher than that of many adsorbents, such as *Artocarpus odoratissimus* skin and leaves, *Azolla pinnata* and others, showing that CMS is more effective in removing MV 2B dye than many reported adsorbents. This makes CMS more effective and attractive as an adsorbent because of its low cost and easy preparation which involved oven drying only. With modification of CMS, the q_{max} was tremendously increased to 670 mg g^{-1}, that is, an increase of approximately 200%, which is a significant achievement of this research.

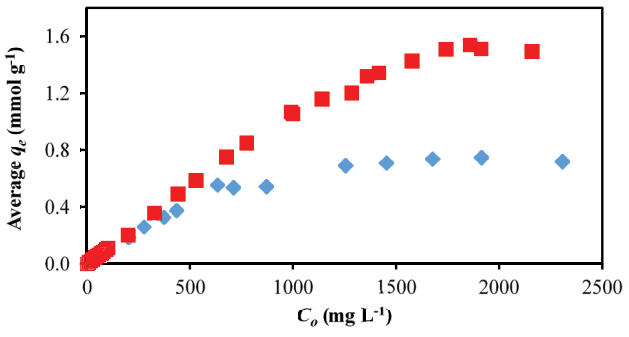

Fig. 3. Isotherm plots of CMS (◆) and MCMS (■).

3.4. Kinetic models

The prediction of the adsorption mechanism can be obtained from analyses using two kinetic models, namely pseudo-first-order [51] and pseudo-second-order [52]. Adsorption process involves the transportation of adsorbate onto the absorbent followed by the diffusion of the adsorbate molecules into the interior of the adsorbent particles. Intraparticle diffusion model was used to investigate on the possibility of the diffusion process of the adsorption. According to Weber and Morris [53], intraparticle diffusion is the rate determining step if the linear plot of Weber–Morris passes through the origin.

Pseudo-first-order kinetics model, first introduced by Lagergren as a simple reversible kinetic process, is stated in Eq. (10) with the linearized equation shown in Eq. (11):

Table 1
Adsorption parameters of all the of isotherm models used

Model	CMS	MCMS
Langmuir		
q_{max} (mmol g^{-1})	0.79	1.92
K_L (L $mmol^{-1}$)	0.01	0.01
R^2	0.9230	0.9582
Freundlich		
K_F (mmol g^{-1} (L $mmol^{-1})^{1/n}$]	0.01	0.02
n	1.43	1.41
R^2	0.9047	0.9212
Temkin		
K_T (L $mmol^{-1}$)	0.06	0.10
b_T (J mol^{-1})	14,351.50	6,928.34
R^2	0.9716	0.9616
D-R		
q_{max} (mmol g^{-1})	0.59	1.14
B (J mol^{-1})	4.83×10^{-6}	2.23×10^{-6}
E (kJ mol^{-1})	321.83	473.24
R^2	0.9838	0.8661
R-P		
K_R (L g^{-1})	0.06	0.03
α	0.31	0.35
a_R (L $mmol^{-1}$)	5.87	0.89
R^2	0.6368	0.6605
Sips		
q_{max} (mmol g^{-1})	0.57	1.70
K_s (L $mmol^{-1}$)	0.00	0.00
$1/n$	1.75	1.21
n	0.57	0.82
R^2	0.9849	0.9817

Table 2
Different error analyses expressions

Error Function	Expression
Average relative error (ARE)	$\frac{100}{n}\sum_{i=1}^{n}\left\lvert\frac{q_{e,\text{meas}}-q_{e,\text{cal}}}{q_{e,\text{meas}}}\right\rvert_i$
Sum square error (EERSQ)	$\sum_{i=1}^{n}\left(q_{e,\text{cal}}-q_{e,\text{meas}}\right)_i^2$
Sum of absolute error (EABS)	$\sum_{i=1}^{n}\left[q_{e,\text{meas}}-q_{e,\text{cal}}\right]$
Hybrid Fractional error function (HYBRID)	$\frac{100}{n-p}\sum_{i=1}^{n}\left[\frac{\left(q_{e,\text{meas}}-q_{e,\text{cal}}\right)^2}{q_{e,\text{meas}}}\right]_i$
Marquardt's percent standard deviation (MPSD)	$\frac{100}{n-p}\sqrt{\frac{1}{n-p}\sum_{i=1}^{n}\left[\frac{q_{e,\text{meas}}-q_{e,\text{cal}}}{q_{e,\text{meas}}}\right]_i^2}$
Chi-square (χ^2)	$\sum_{i=1}^{n}\left[\frac{\left(q_{e,\text{meas}}-q_{e,\text{cal}}\right)^2}{q_{e,\text{meas}}}\right]_i$

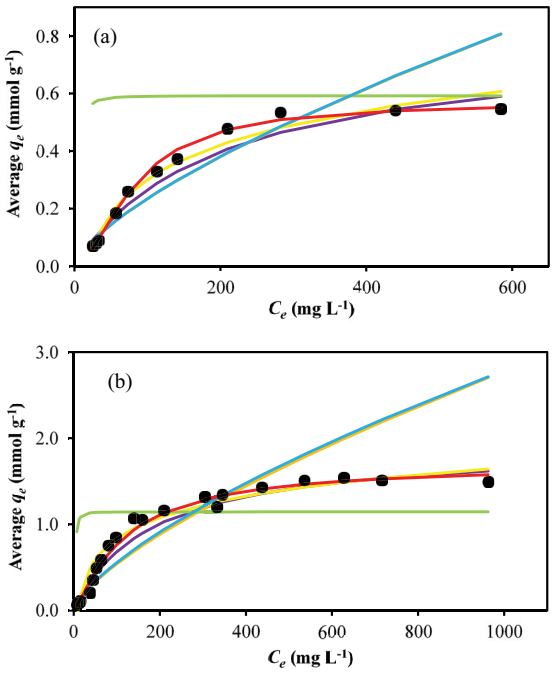

Fig. 4. Adsorption isotherm data of (a) CMS and (b) MCMS with various simulated isotherm models [Experiment (●), Langmuir (—), Freundlich (—), Temkin (—), D-R (—), R-P (—), and Sips (—)].

Table 3
Error analysis of various isotherm models used in adsorption of MV 2B dye onto CMS and MCMS

Model	R^2	ARE	EERSQ	HYBRID	EABS	MPSD	χ^2
CMS							
Langmuir	0.9230	15.05	0.017	0.67	0.39	19.47	0.06
Freundlich	0.9047	23.06	0.109	2.64	0.82	27.46	0.24
Temkin	0.9716	9.82	0.011	0.33	0.27	12.59	0.03
D-R	0.9838	218.78	1.135	120.98	2.96	372.97	10.89
R-P	0.6368	22.88	0.109	2.97	0.81	23.55	0.24
Sips	0.9849	4.65	0.003	0.11	0.13	7.20	0.01
MCMS							
Langmuir	0.9582	15.96	0.24	1.65	1.85	22.46	0.33
Freundlich	0.9212	27.96	2.79	10.88	5.09	34.04	2.18
Temkin	0.9616	36.90	0.26	6.59	1.89	81.26	1.32
D-R	0.8661	297.93	7.43	288.24	10.59	558.87	57.65
R-P	0.6605	26.57	2.83	11.41	5.05	33.78	2.17
Sips	0.9817	11.01	0.09	0.87	1.08	18.09	0.16

$$\frac{dq_t}{dt}=K_1\left(q_e-q_t\right) \tag{10}$$

$$\log\left(q_e-q_t\right)=\log\left(q_e\right)-\frac{K_1}{2.303}t \tag{11}$$

Pseudo-second-order kinetic model, developed by Ho and McKay [52], is given in Eq. (12) with the linearized equation in Eq. (13):

$$\frac{dq_t}{dt}=k_2\left(q_e-q_t\right)^2 \tag{12}$$

$$\frac{t}{q_t}=\frac{1}{h}+\frac{1}{q_e}t \tag{13}$$

Intraparticle diffusion model was developed by Weber and Morris to discuss on the diffusion adsorption kinetics.

Table 4
Comparison of maximum adsorption capacity of different adsorbents used on the removal of MV 2B dyes

Adsorbents	q_{max} (mg g^{-1})	Reference
Cucumis melo var. cantalupensis skin	224.6	This work
Cempedak durian peel (CDP)	238.5	[13]
Artocarpus odoratissimus (Tarap) skin	137.3	[30]
A. odoratissimus leaves	139.7	[22]
Extracted cellulose of *A. odoratissimus* leaves	187.0	[31]
Halloysite nanotubes	113.6	[32]
Azolla pinnata	194.2	[33]
HNT-Fe_3O_4 composite	20.0	[34]
Fe_3O_4 magnetic nanoparticles	416.7	[35]
Casuarina equisetifolia needle	165.0	[36]
Casuarina equisetifolia cone	63.0	[37]
Pomelo skin	468.3	[38]
Nepenthes rafflesiana pitcher	288.7	[39]
Pistia stratiotes L. (water lettuce)	267.6	[40]
Halloysite-magnetite-based composite	20.0	[34]
Polyacrylamide grafted xanthan gum with nanosilica	378.8	[41]
Lemna minor (Duckweed)	332.5	[42]
Artocarpus heterophyllus (jackfruit) seed	126.7	[43]
Pu-erh tea powder (40 mesh)	277.8	[44]
Pomelo leaves	248.2	[45]
Artocarpus odoratissimus stem axis	263.7	[46]
Modified *Cucumis melo var. cantalupensis* skin	669.7	This work
Acid modified *S. bengalense*	7.3	[47]
Acid modified activated carbon	83.3	[48]
Base modified *Artocarpus odoratissimus* leaves	1004.3	[22]
Salvadora oleoides	58.5	[49]
Microwave treated *Salvadora oleoides*	219.7	[49]
Ammonium sulfide hydrothermal activated Palygorskite	218.1	[50]

The linear expression of intraparticle diffusion model is shown in Eq. (14) below:

$$q_t = k_3 t^{1/2} + C \tag{14}$$

Comparison made between the experimental data and the pseudo-first and second-order kinetics where the simulation plots for both the CMS and MCMS, as shown in Figs. 5a and b, respectively, indicated that the pseudo-second-order model was closer to the experimental data.

This is further confirmed by the linear plots of both models (Fig. 6) where the R^2 values of CMS and MCMS for pseudo-second kinetics are near unity. Values of the error analyses of pseudo-second-order were also the lowest as compared with those of the pseudo-first-model (Table 5). Further confirmation was based on the experimental values of adsorption capacity, q_e, of CMS (0.372 mmol g^{-1}) and MCMS (0.587 mmol g^{-1}) which are closest to the q_{cal} of 0.512 and 0.579 mmol g^{-1}, respectively.

According to the Weber–Morris intraparticle diffusion model, if the linear plot of q_e vs. $t^{1/2}$ passes through the origin, the reaction is controlled by intraparticle diffusion. As shown in Figs. 6c and d, none of the linear plots passes through the origin suggesting that intraparticle diffusion is not the rate determining step of the adsorption of MV 2B by both CMS and MCMS.

3.5. Effect of ionic strength

Interactions between the charged salts, adsorbents and adsorbates would influence the adsorption capacity of an adsorbent. Effect of ionic strength investigated in this study shows a decreasing trend of removal ability as the concentration of the salt in the solution increased (Fig. 7). This is probably due to the presence of positively charged K^+ and Na^+ ions competing with the cationic dyes (MV 2B) for the active sites of the adsorbents, leading to the reduction of the adsorption capacity of the adsorbents, hence the removal of MV 2B dye was lower. According to Fig. 7, the removal ability of the CMS decreased drastically with the increase in salt concentration from approximately 70% to 10% in the presence of 1 M salt. The percentage removal of the dye in the presence of the four salts, namely, NaCl, $NaNO_3$, KCl and KNO_3 decreased from an average of 72% (in the absence of salt) to 48%, 11%, 30% and 7%, respectively. The concentration of KNO_3 affected the adsorption of MV 2B dye the most. The percentage removal

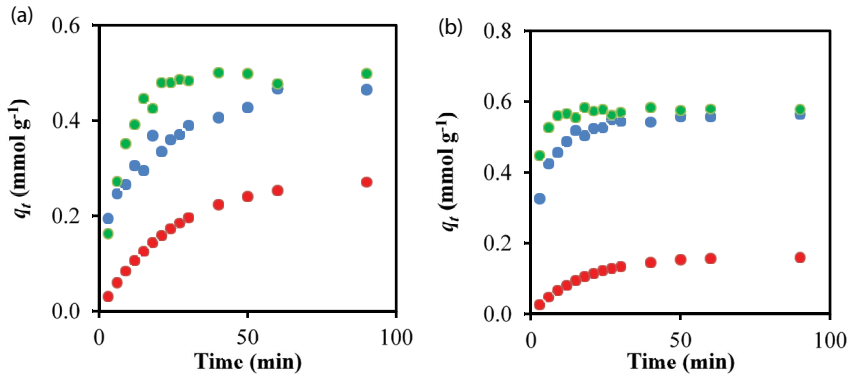

Fig. 5. Simulation plots of pseudo-first (●) and pseudo-second (●) order kinetic models with the experimental data (●) of (a) CMS and (b) MCMS.

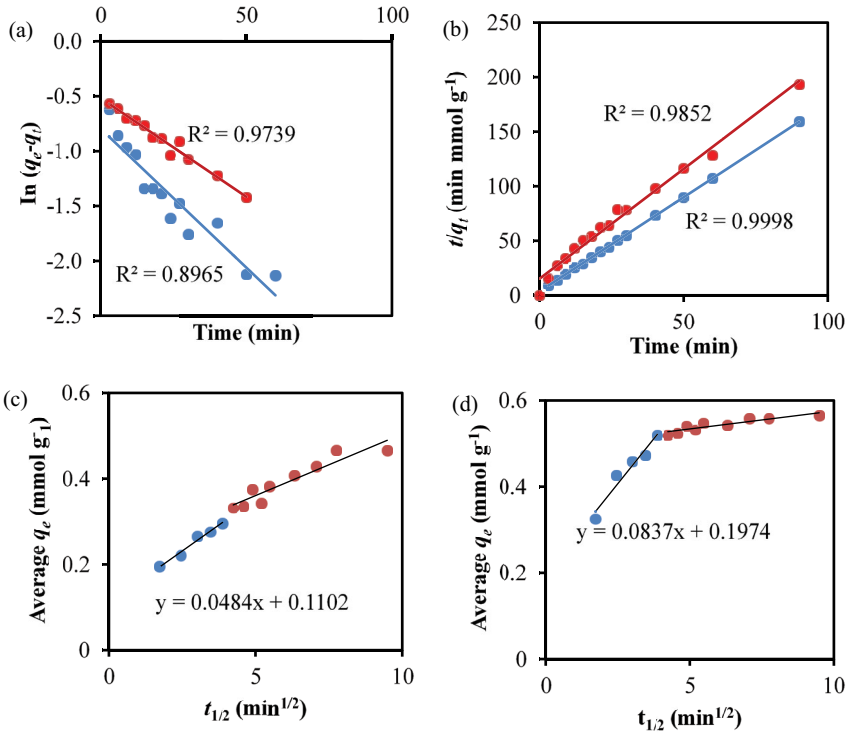

Fig. 6. Plotted kinetics of (a) pseudo-first-order and (b) pseudo-second-order kinetics of CMS (●) and MCMS (●) with the intraparticle diffusion plots of (c) CMS and (d) MCMS.

of MV 2B dye by MCMS was initially 83% and reduced to 76%, 52%, 75% and 45% in the presence of NaCl, $NaNO_3$, KCl and KNO_3, respectively. When comparing both the adsorbents, the adsorption efficiency of MCMS was not affected as much as CMS was. The possible reason could be that the surface of MCMS was predominately hydroxyl ions charged which increased the active site for both positively charged salt (K^+ and Na^+) and cationic dye (MV 2B), reduced competition on the active sites among the two sources.

3.6. Regeneration studies

It is not only cost-effective but also time consuming if spent adsorbents were able to be recycled, yet maintaining high adsorption capacity. The overall trend for both CMS and MCMS showed that the effectiveness of the adsorption decreased with increased number of cycles (Figs. 8a and b). Among many regeneration methods attempted, the most effective method to regenerate adsorbents was by washing with acid and base. This is because acid and base washing can further enhance the adsorption capacity by modifying the surface of the adsorbent. The percentage removals of MV 2B dye by acid and base treatment were reduced by approximately 25% and 40%, respectively. However, base treatment on MCMS did not show a good recovery compared with CMS after five cycles of adsorption–desorption process. This is possibly because the MCMS was already initially modified with base, therefore the effect of surface modification is

Table 5
Comparison q_{cal} with q_e (in mmol g^{-1}), rate constant and error analyses of CMS and MCMS between pseudo-first-order and pseudo-second-order

			R^2	ARE	EERSQ	HYBRID	EABS	MPSD	χ^2
CMS									
Pseudo-first-order	q_{cal} = 0.3050	k_1 (min^{-1}) = 0.4150	0.7187	56.51	0.50	12.39	2.65	62.44	1.49
Pseudo-second-order	q_{cal} = 0.5121	k_2 (g $mmol^{-1}$ min^{-1}) = 0.2098	0.9922	23.98	0.12	2.86	1.12	29.54	0.34
	q_e = 0.3719								
MCMS									
Pseudo-first-order	q_{cal} = 0.1607	k_1 (min^{-1}) = 0.0583	0.7187	79.01	2.21	36.40	5.55	85.60	4.37
Pseudo-second-order	q_{cal} = 0.5794	k_2 (g $mmol^{-1}$ min^{-1}) = 0.7899	0.9998	11.93	0.06	1.15	0.76	16.78	0.14
	q_e = 0.5870								

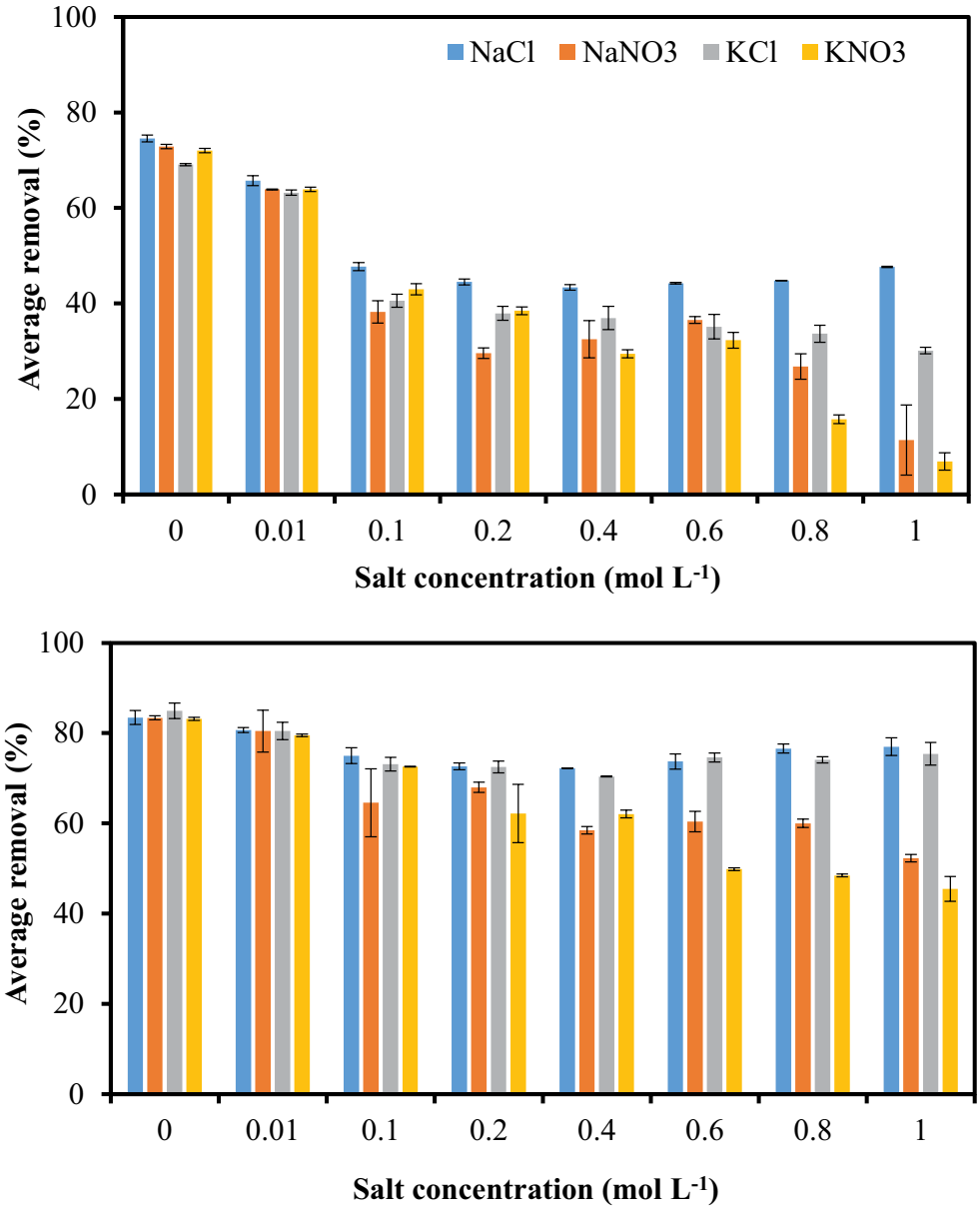

Fig. 7. Effect of ionic strengths on CMS (top) and MCMS (below) using NaCl (■), $NaNO_3$ (■), KCl (■) and KNO_3 (■).

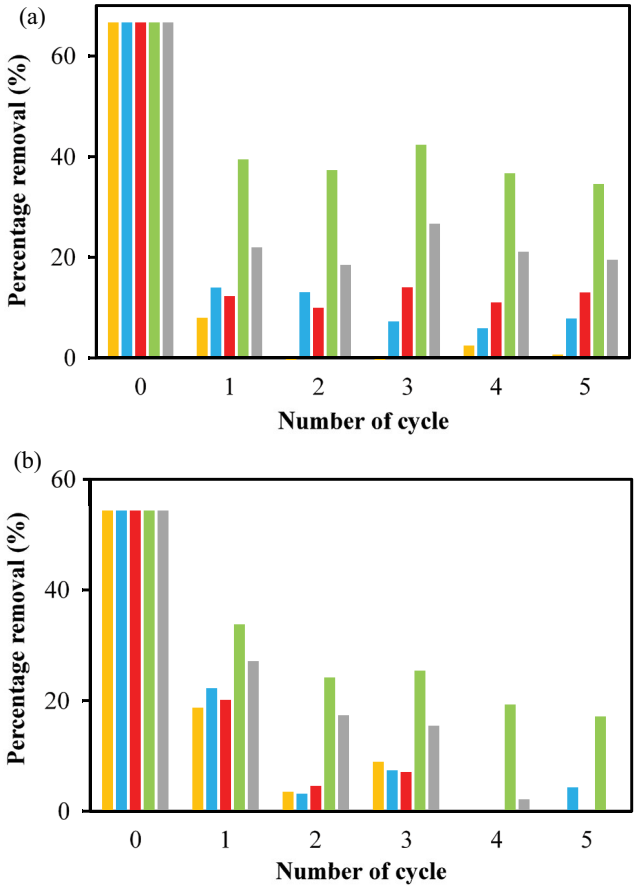

Fig. 8. Cycles of adsorption–desorption process of MV 2B dye (800 mg L^{-1}) on (a) CMS and MV 2B dye (2,000 mg L^{-1}) on (b) MCMS using quick wash (■), distilled water (■), acid (■), base (■) and control (■).

not as significant. However, acid treatment showed a higher restoration among other treatment methods with an overall reduction of 35% after five cycles. Although the adsorption of dyes on both CMS and MCMS showed a reduction after a few cycles, it still maintained a good adsorption even after five cycles. Despite the observed reduction, it has to be highlighted that the concentrations of dye used were much higher than compared with most reported studies. Hence, both adsorbents are considered regenerable and reusable.

3.7. Characterizations of the adsorbents

3.7.1. Point of zero charge

Point of zero charge (pH_{pzc}), the pH at which the surface of the adsorbent has a net charge of zero [22], determined from the graph of change in pH (initial pH–final pH) vs. initial pH, indicates that the pH_{pzc} values of CMS and MCMS are at pH 7.2 and 6.6, respectively (Fig. 9). Below the pH_{pzc}, the surface of the adsorbent is predominantly positively charged favoring the adsorption of adsorbate on the negative charged surface. When solution pH is higher than pH_{pzc}, the surface of the adsorbent would be predominantly negatively charged, favoring the adsorption of positively charged adsorbate [22]. Since MV 2B is a cationic dye, optimum pH for adsorption

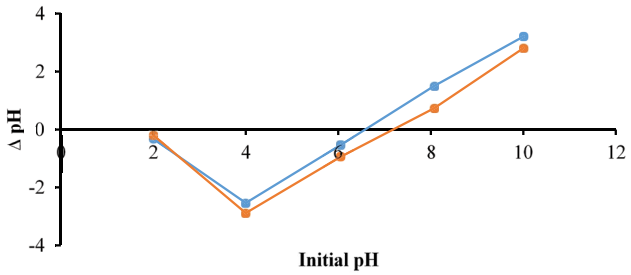

Fig. 9. Point of zero charges of CMS (■) and MCMS (■).

should be higher than 7.2 and 6.6 for CMS and MCMS, respectively.

3.7.2. Scanning electron microscopy

Figs. 10a and b show the surface morphology of CMS and MCMS, while Figs. 10c and d show their surface after adsorption with MV 2B dye, respectively. It is observed from the images that the surface of MCMS have more folds and is more porous than CMS, indicating that the surface area of MCMS is larger which allows more adsorption of MV 2B dye onto the surface. This further demonstrates enhanced adsorption capacity of MCMS toward MV 2B dye than that of CMS.

3.7.3. Fourier transform infrared (FT-IR) spectroscopy

Fig. 11a shows the comparison of IR spectra of MCMS and CMS. The peak of 3,269 cm^{-1} is representing O–H hydroxyl group and N–H bond of CMS. Upon surface modification with base, this was shifted to 3,285 cm^{-1} for MCMS. There is also a noticeable shift of peak of C–H stretching from 2,922 and 2,853 cm^{-1} (CMS) to 2,916 and 2,849 cm^{-1} (MCMS), respectively. The functional group of C=C bond of aromatic is corresponding to peak at 1,617 cm^{-1} for CMS and 1,582 cm^{-1} for MCMS. Peak at 1,026 and 1,004 cm^{-1} show the appearance of C–O ester bond for CMS and MCMS, respectively. These shifting of peak positions indicate that modification of CMS cause changes to the functional groups of the MCMS's surface.

The IR spectra of CMS and adsorption of dye onto CMS are shown in Fig. 11b. The peak appears at 3,268 cm^{-1} is corresponding to O–H hydroxyl group and N–H bond. Peaks of 2,921 and 2,853 cm^{-1} are representing C–H stretching. The peak at 1,617 cm^{-1} shows that C=C bond of aromatic presence on the surface of CMS. C–O stretching is representing by the appearance of 1,030 cm^{-1} peak. After adsorption of MV 2B dyes, the peak of –OH and N–H group shifted from 3,268 to 3,264 cm^{-1}. There is also a noticeable shift of peak from 1,617 to 1,582 cm^{-1} corresponding to the C=C bond interaction. A slight shift of peak from 1,030 to 1,026 cm^{-1} was observed which represent the C–O interaction with MV 2B dye. Hence, –OH group, N–H bond, C=C bond and C–O bond are responsible for the adsorption of MV 2B dyes.

The IR spectra of MCMS before and after adsorption of dye are shown in Fig. 11c. A peak appears at 3,284 cm^{-1} is corresponding to the O–H and N–H group. At wave number of 2,916 and 2,850 cm^{-1}, the peaks are representing C–H

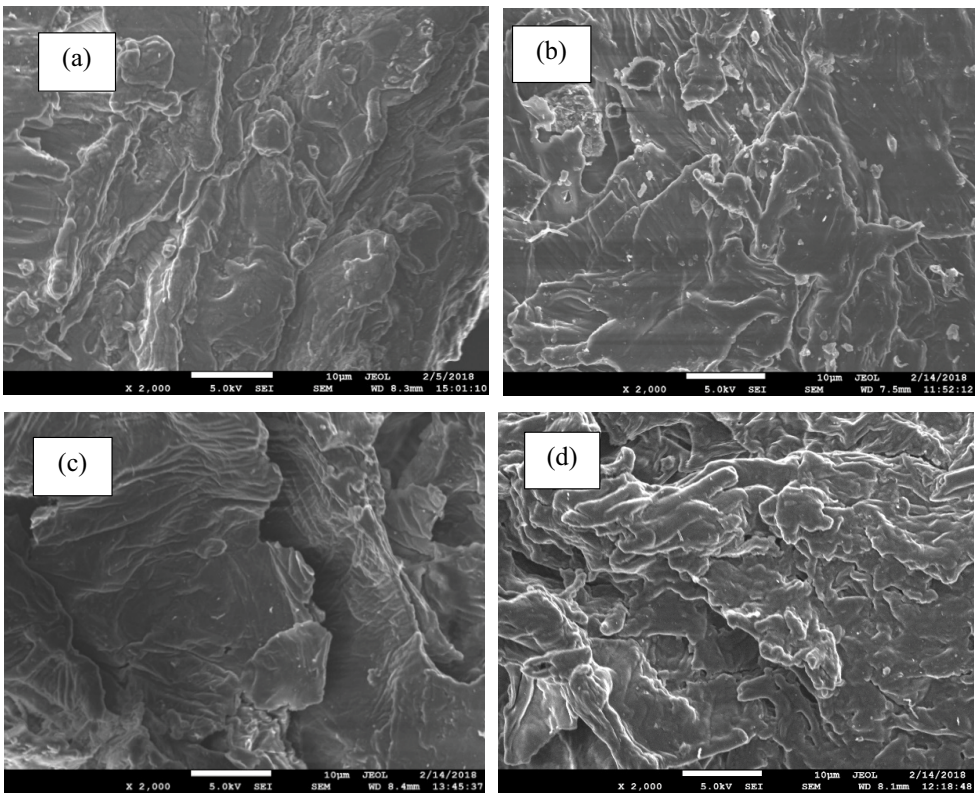

Fig. 10. SEM images showing surface morphology of (a) CMS (b) MCMS (c) CMS loaded with dye and (d) MCMS with dye.

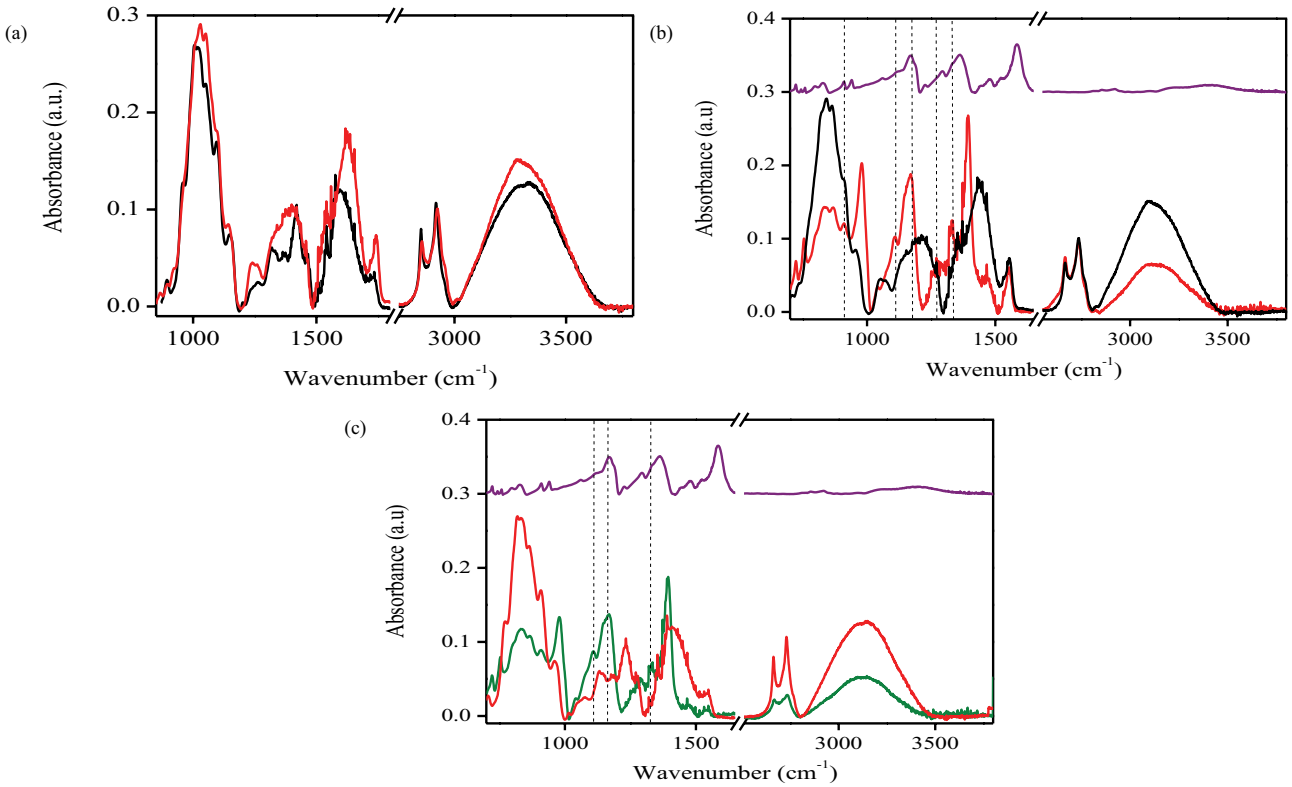

Fig. 11. FTIR spectra of (a) CMS (—) and MCMS (—) (b) CMS (—), CMS loaded with dye (—) and the dye itself (—) while (c) MCMS (—), MCMS loaded with dye (—) and the dye itself (—).

stretching. The peaks at 1,582 and 1,420 cm^{-1} indicate the presence of C=C aromatic bond, while the C–O bond of ester is shown by the peak at 1,005 cm^{-1}. The adsorption of dye onto MCMS results in slight shifts in the peak positions. Peak of O–H stretching and N–H group shifted from 3,284 to 3,277 cm^{-1}. The interaction of C–H stretching also results in shifting of peaks from 2,916 and 2,850 cm^{-1} to 2,920 and 2,863 cm^{-1}, respectively. The C=C aromatic bond was also shifted from 1,420 to 1,356 cm^{-1}. The peak of ester C–O bond shifted from 1,004 to 1,028 cm^{-1}. Therefore, the functional groups of MCMS responsible for the interaction with MV 2B dyes are O–H, N–H, C–H, C=C aromatic groups and C–O ester bond.

4. Conclusion

Investigation on the efficiency of rock melon skin and its base-modified form as new adsorbents in removing MV 2B dye was successfully carried out in this study. The adsorbent–adsorbate system reached equilibrium in 1.5 h. Base modification of CMS using 1 M NaOH showed an enhancement by almost 200% where q_{max} increased from 224.56 to 669.73 mg g^{-1}, toward MV 2B dye, with the Sips adsorption isotherm being the best model to describe the adsorption of MV 2B dye onto CMS and MCMS. Adjusting medium pH was not necessary as the effect of dye removal at ambient pH and at pH with the highest extent of removal was comparable. Experimental data indicated that the adsorption kinetics of CMS and MCMS followed the pseudo-second-order model. The adsorption ability of MCMS was not affected as much as that of CMS in the presence of salts. Regeneration of MCMS is potentially higher when washed with acid. Therefore, CMS and MCMS both have the potential to be used as new adsorbents to remove MV 2B dye in the wastewater treatment.

Acknowledgments

The authors would like to express their appreciation to the Government of Negara Brunei Darussalam and the Universiti Brunei Darussalam (UBD) for their support. Their appreciations also go to the Physical and Geological Sciences Department and Centre for Advanced Material and Energy Sciences (CAMES) for the use of SEM and FTIR, respectively.

References

[1] M. Shahbaz, S.J.H. Shahzad, M.K. Mahalik, S. Hammoudeh, Does globalisation worsen environmental quality in developed economies?, Environ. Model. Assess., 1–8 (2018) 141–156.
[2] M. Gavrilescu, K. Demnerová, J. Aamand, S. Agathos, F. Fava, Emerging pollutants in the environment: present and future challenges in biomonitoring, ecological risks and bioremediation, New Biotechnol., 32 (2015) 147–156.
[3] A.E. Ghaly, R. Ananthashankar, M.V.V.R. Alhattab, V.V. Ramakrishnan, Production, characterization and treatment of textile effluents: a critical review, J. Chem. Eng. Process Technol., 5 (2014) 1–19.
[4] S. Dey, A. Islam, A review on textile wastewater characterization in Bangladesh, Res. Environ., 5 (2015) 15–44.
[5] P.U. Singare, S.S. Dhabarde, Pollution due to textile industries along Dombivali Industrial Belt of Mumbai, India, Int. Letters Chem. Phys. Astronomy, 3 (2014) 24–31.
[6] A. Hasanbeigi, L. Price, A technical review of emerging technologies for energy and water efficiency and pollution reduction in the textile industry, J. Clean. Prod., 95 (2015) 30–44.
[7] E.A. Sweeney, J.K. Chipman, S.J. Forsythe, Evidence for direct-acting oxidative genotoxicity by reduction products of azo dyes, Environ. Health Persp., 102 (1994) 119–122.
[8] A. Gottlieb, C. Shaw, A. Smith, A. Wheatley, S. Forsythe, The toxicity of textile reactive azo dyes after hydrolysis and decolourisation, J. Biotechnol., 101 (2003) 49–56.
[9] F. Copaciu, O. Opriş, V. Coman, D. Ristoiu, Ü. Niinemets, L. Copolovici, Diffuse water pollution by anthraquinone and azo dyes in environment importantly alters foliage volatiles, carotenoids and physiology in wheat (Triticum aestivum), Water Air Soil Pollut., 224 (2013) 1478–1489.
[10] K. Schneider, C. Hafner, I. Jäger, Mutagenicity of textile dye products, J. Appl. Toxicol., 24 (2004) 83–91.
[11] M.A. Hassaan, A. El Nemr. Health and environmental impacts of dyes: mini review, Am. J. Envrion. Sci. Eng., 1 (2017) 64–67.
[12] Markandeya, S.P. Sukhla, D. Mohan, Toxicity of disperse dyes and its removal from wastewater using various adsorbents: a review, Res. J. Environ. Toxic., 11 (2017) 72–89.
[13] M.K. Dahri, H.I. Chieng, L.B.L. Lim, N. Priyantha, C.C. Mei, Cempedak durian (Artocarpus sp.) peel as a biosorbent for the removal of toxic methyl violet 2B from aqueous solution, Korean Chem. Eng. Res., 53 (2015) 576–583.
[14] K. Jeyasubramanian, G.S. Hikku, R.K. Sharma, Photo-catalytic degradation of methyl violet dye using zinc oxide nano particles prepared by a novel precipitation method and its anti-bacterial activities, J. Water Process Eng., 8 (2015) 35–44.
[15] L.B.L. Lim, N. Priyantha, N.A.H.M. Zaidi, U.A.N. Jamil, H.I. Chieng, T. Zehra, A. Liyandeniya, Chemical modification of Artocarpus odoratissimus skin for enhancement of their adsorption capacities toward toxic malachite green dye, J. Mater. Environ. Sci., 7 (2016) 3211–3224.
[16] S.W. Choi, D.-H. Lee, J. Kim, J. Kim, J.-H. Park, H.T. Beum, D.-S. Lim, K.B. Lee, A titanium carbide-derived novel tetrafluoromethane adsorbent with outstanding adsorption performance, Chem. Eng. J., 311 (2017) 227–235.
[17] S.J. Nielsen, L.M. Rossen, D.M. Harris, C.L. Ogden, Fruit and vegetable consumption of US Youth, 2009–2010, NCHS. Data Brief, 23 (2018) 141–156.
[18] H.I. Chieng, L.B.L. Lim, N. Priyantha, Enhancing adsorption capacity of toxic malachite green dye through chemically modified breadnut peel: equilibrium, thermodynamics, kinetics and regeneration studies, Environ. Technol., 36 (2015) 86–97.
[19] L.B.L. Lim, N. Priyantha, T. Zehra, C.W. Then, C.M. Chan, Adsorption of crystal violet dye from aqueous solution onto chemically treated Artocarpus odoratissimus skin: equilibrium, thermodynamics, and kinetics studies, Desal. Wat. Treat., 57 (2016) 10246–10260.
[20] H.I. Chieng, L.B.L. Lim, N. Priyantha, Enhancement of crystal violet dye adsorption on Artocarpus camansi peel through sodium hydroxide treatment, Desal. Wat. Treat., 58 (2017) 320–331.
[21] M.K. Dahri, L.B.L. Lim, M.R.R. Kooh, C.M. Chan, Adsorption of brilliant green from aqueous solution by unmodified and chemically modified Tarap (*Artocarpus odoratissimus*) peel, Int. J. Environ. Sci. Technol., 14 (2017) 2683–2694.
[22] L.B.L. Lim, N. Priyantha, N.A.H.M. Zaidi, A superb modified new adsorbent, Artocarpus odoratissimus leaves, for removal of cationic methyl violet 2B dye, Environ. Earth Sci., 75 (2016) 1179.
[23] S. Cengiz, L. Cavas, A promising evaluation method for dead leaves of *Posidonia oceanica* (L.) in the adsorption of methyl violet, Marine Biotechnol., 12 (2010) 728–736.
[24] I. Langmuir, The adsorption of gases on plane surfaces of glass, mica and platinum, J. Am. Chem. Soc., 40 (1918) 1361–1403.
[25] H. Freundlich, Over the adsorption in the solution, J. Phys. Chem., 57 (1906) 385–470.
[26] M. Temkin, V. Pyzhev, Kinetics of ammonia synthesis on promoted iron catalyst, Acta Phys. Chim. USSR, 12 (1940) 327–356.
[27] M.M. Dubinin, L.V. Radushkevich, The equation of the characteristic curve of the activated charcoal, Proc. Acad. Sci. USSR. Phys. Chem. Sec., 55 (1947) 331–337.
[28] O. Redlich, D.L. Peterson, A useful adsorption isotherm, J. Phys. Chem., 63 (1959) 1024–1024.

[29] R. Sips, On the structure of a catalyst surface, J. Chem. Phys., 16 (1948) 490–495.
[30] L.B.L. Lim, N. Priyantha, C. Hei Ing, M. Khairud Dahri, D.T.B. Tennakoon, T. Zehra, M. Suklueng, Artocarpus odoratissimus skin as a potential low-cost biosorbent for the removal of methylene blue and methyl violet 2B, Desal. Wat. Treat., 53 (2015) 964–975.
[31] N.A.H.M. Zaidi, L.B.L. Lim, A. Usman, Artocarpus odoratissimus leaf-based cellulose as adsorbent for removal of methyl violet and crystal violet dyes from aqueous solution, Cellulose, 25 (2018) 3037–3049.
[32] R. Liu, B. Zhang, D. Mei, H. Zhang, J. Liu, Adsorption of methyl violet from aqueous solution by halloysite nanotubes, Desalination, 268 (2011) 111–116.
[33] M.R.R. Kooh, L.B.L. Lim, M.K. Dahri, L.H. Lim, J.M.R.S. Bandara, Azolla pinnata: an efficient low cost material for removal of methyl violet 2B by using adsorption method, Waste Biomass Valor., 6 (2015) 547–559.
[34] L.R. Bonetto, F. Ferrarini, C. De Marco, J.S. Crespo, R. Guégan, M. Giovanela, Removal of methyl violet 2B dye from aqueous solution using a magnetic composite as an adsorbent, J. Water Process Eng., 6 (2015) 11–20.
[35] F. Keyhanian, S. Shariati, M. Faraji, M. Hesabi, Magnetite nanoparticles with surface modification for removal of methyl violet from aqueous solutions, Arab. J. Chem., 9 (2016) S348–S354.
[36] M.K. Dahri, M.R.R. Kooh, L.B.L. Lim, Removal of methyl violet 2B from aqueous solution using Casuarina equisetifolia needle, ISRN Environ. Chem., 2013 (2013) 619819.
[37] M.K. Dahri, M.R.R. Kooh, L.B.L. Lim, Water remediation using Casuarina equisetifolia cone as adsorbent for the removal of methyl violet 2B dye using batch experiment method, J. Environ. Biotechnol. Res., 6 (2017) 34–42.
[38] M.K. Dahri, M.R.R. Kooh, L.B.L. Lim, Artificial neural network approach for modelling of methyl violet 2B dye adsorption using pomelo skin, J. Environ. Biotechnol. Res., 6 (2017) 238–247.
[39] M.R.R. Kooh, M.K. Dahri, L.B.L. Lim, Removal of methyl violet 2B dye from aqueous solution using Nepenthes rafflesiana pitcher and leaves, Appl. Water Sci., 7 (2017) 3859–3868.
[40] L.B.L. Lim, N. Priyantha, C.M. Chan, D. Matassan, H.I. Chieng, M.R.R. Kooh, Investigation of the sorption characteristics of water lettuce (WL) as a potential low-cost biosorbent for the removal of methyl violet 2B, Desal. Wat. Treat., 57 (2016) 8319–8329.
[41] S. Ghorai, A. Sarkar, M. Raoufi, A.B. Panda, H. Schönherr, S. Pal, Enhanced removal of methylene blue and methyl violet dyes from aqueous solution using a nanocomposite of hydrolyzed polyacrylamide grafted xanthan gum and incorporated nanosilica, ACS Appl. Mater. Interface, 6 (2014) 4766–4777.
[42] L.B.L. Lim, N. Priyantha, C.M. Chan, D. Matassan, H.I. Chieng, M.R.R. Kooh, Adsorption behavior of methyl violet 2B using duckweed: equilibrium and kinetics studies, Arab. J. Sci. Eng., 39, (2014) 6757–6765.
[43] M.K. Dahri, M.R.R. Kooh, L.B.L. Lim, Adsorption of toxic methyl violet 2B dye from aqueous solution using Artocarpus heterophyllus (Jackfruit) seed as an adsorbent, Am. Chem. Sci. J., 15 (2016) 1–12.
[44] P. Li, Y.-J. Su, Y. Wang, B. Liu, L.-M. Sun, Bioadsorption of methyl violet from aqueous solution onto Pu-erh tea powder, J. Harzard. Mater., 179 (2010) 43–48.
[45] L.B.L. Lim, N. Priyantha, Y.C. Lu, N.A.H.M. Zaidi, Effective removal of methyl violet dye using pomelo leaves as a new low-cost adsorbent, Desal. Wat. Treat., 110 (2018) 264–274.
[46] M.R.R. Kooh, M.K. Dahri, L.B.L. Lim, Removal of the methyl violet 2B dye from aqueous solution using sustainable adsorbent Artocarpus odoratissimus stem axis, Appl. Water Sci., 7 (2017) 3573–3581.
[47] M.I. Din, K. Ijaz, K. Naseem, Biosorption potentials of acid modified Saccharum bengalense for removal of methyl violet from aqueous solutions, Chem. Ind. Chem. Eng. Quart., 23 (2017) 399–409.
[48] A.T.M. Din, B.H. Hameed, Adsorption of methyl violet dye on acid modified activated carbon: isotherms and thermodynamics, J. Appl. Sci. Environ. Sanit., 5 (2010) 161–170.
[49] M.I. Din, Z. Hussain, H. Munir, A. Naz, A. Intisar, M.N. Makshoof, M.L. Mirza, Microwave treated Salvadora oleoides as an eco-friendly biosorbent for the removal of toxic methyl violet dye from aqueous solution—a green approach, Int. J. Phytoremed., 18 (2016) 477–486.
[50] G. Tian, W. Wang, Y. Kang, A. Wang, Ammonium sulfide-assisted hydrothermal activation of palygorskite for enhanced adsorption of methyl violet, J. Environ. Sci., 41 (2016) 33–43.
[51] S. Lagergren, About the theory of so-called adsorption of soluble substances, K. Sven. Vetenskapsakad. Handl., 24 (1898) 1–39.
[52] Y.S. Ho, G. McKay, Sorption of dye from aqueous solution by peat, Chem. Eng. J., 70 (1998) 115–124.
[53] W.J. Weber, J.C. Morris, Kinetics of adsorption on carbon from solution, J. Sanit. Eng. Div., 89 (1963) 31–60.